DALTON
FULL PAPER

Computational study of the geometric and electronic structures of MN_2 (M = Mo or U)

Katherine L. Brown and Nikolas Kaltsoyannis

Department of Chemistry, University College London, 20 Gordon Street, London, UK WC1H 0AJ. E-mail: n.kaltsoyannis@ucl.ac.uk; web: http://calcium.chem.ucl.ac.uk/webstuff/people/nkalt/index.html

Received 30th September 1999, Accepted 1st November 1999

The geometric and electronic structures of singlet, triplet, quintet and septet MN_2 (M = Mo or U) have been calculated using quasi-relativistic, non-local density functional theory. The distribution of the MoN_2 structures over the spin states agrees well with previous theoretical data, as do the relative energies and vibrational wavenumbers of the minima. Six true minimum energy stationary point UN_2 structures have been located. Whereas all of the MoN_2 structures are less stable than the Mo + N_2 asymptote, all of the UN_2 minima are stable with respect to dissociation to metal + dinitrogen. Singlet linear NUN is found to be the most stable UN_2 structure at the scalar relativistic level, and the inclusion of spin–orbit coupling does not significantly affect the NUN energy with respect to the U + N_2 asymptote. The bonding in all of the UN_2 structures has been analysed. The U–N_2 interaction in the quintet and septet narrow angle side-on triangular geometries is a mixture of U 5f→N_2 π_g δ and π backbonding, with the latter component being much the more significant. U→N_2 π backbonding is also found to be the principal U–N_2 interaction in triplet and septet linear end-on UN_2. The U–N Mulliken overlap populations are largest for the wide angle triangular and linear NUN structures, consistent with the much shorter U–N bond lengths in these geometries in comparison with the narrow angle side-on and linear end-on minima. The agreement between the calculated and experimental vibrational wavenumbers for linear NUN is very good, and is superior to previous theoretical studies. The relevance of the present work to previous computational investigations of the U–N_2–U bonding in $[\{(NH_2)_3(NH_3)U\}_2(\mu\text{-}\eta^2:\eta^2\text{-}N_2)]$ is discussed.

Introduction

The last few years have seen a number of important publications describing the synthesis, characterisation and study of d- and f-element complexes in which dinitrogen functions as a ligand to the metal centre(s). Among the transition series, Mo,[1,2] V[3] and Zr[4] have received particular attention, and Sm,[5] Pr and Nd[6] and U[7,8] dinitrogen compounds are now well established. Reference 8 is particularly significant as the diuranium triamidoamine dinitrogen compound that it reports is the first fully characterised N_2 complex of an actinide element.

In an attempt to understand the bonding within the U–N_2–U core of the triamidoamine complex described in reference 8, we conducted a series of density functional calculations on the model compound $[\{(NH_2)_3(NH_3)U\}_2(\mu\text{-}\eta^2:\eta^2\text{-}N_2)]$.[9] This study led us to the conclusion that the U–N_2–U core is held together almost exclusively by U→N_2 π backbonding, an unusual bonding mode for actinide elements, particularly in medium to high oxidation states. This conclusion is not without its problems, however, as the experimental N–N distance is essentially the same as in free dinitrogen,[8] inconsistent with the backbonding model. The plot is further thickened by the fact that computational geometry optimisations on our model complexes always result in N–N lengthening, by an amount dependent in part upon the molecular spin state.[10]

In order to probe more fully the bonding of N_2 to U, we have removed the computational models for the triamidoamine ligands and have reduced the problem to one involving only three atoms. This paper reports the results of quasi-relativistic, non-local density functional theory (DFT) calculations of the geometric and electronic structures of UN_2 in a variety of spin states, together with analyses of the bonding within these complexes. While we accept that UN_2 is considerably different from the experimentally characterised compounds discussed above, our hope is that if we can first understand the interaction of an N_2 molecule with a bare U atom we will be better placed to understand the bimetallic triamidoamine complexes.

We have also studied the analogous MoN_2 system and our findings are reported in this paper. These calculations serve two main purposes. First, MoN_2 has recently been studied computationally by two other groups,[11,12] thereby giving us the opportunity to test our methodology before embarking on the potentially more complicated actinide system. Second, the valence electronic configuration of Mo and U is similar in that both elements have six electrons outside of an inert gas core (Mo: $[Kr]4d^55s^1$, U: $[Rn]5f^36d^17s^2$) and thus MoN_2 and UN_2 have the same range of possible spin states. It was our hope that useful information could be derived from comparisons between the transition metal and actinide systems.

Computational details

All calculations were performed with the Amsterdam Density Functional (ADF) program suite.[13,14] An uncontracted triple-zeta Slater-type orbital valence basis set was employed for all atoms, supplemented with d and f polarisation functions for N (ADF Type V). No polarisation functions were included for Mo or U (ADF Type IV). Quasi-relativistic[15] scalar corrections (Darwin and mass-velocity) were included *via* the Pauli formalism, in which the first-order scalar relativistic Pauli Hamiltonian is diagonalised in the space of the non-relativistic basis sets. Quasi-relativistic frozen cores were computed for all atoms, N(1s), Mo(3d), U(5d), using the ADF auxiliary programme 'Dirac'. The local density parameterisation of Vosko, Wilk and Nusair[16] was employed in conjunction with Becke's gradient correction[17] to the exchange part of the potential and the correlation correction due to Perdew.[18] All of the singlet states reported in this work are closed shell, and the spin

Table 1 Molecular structures, relative energies, spin states, symmetries, valence electronic configurations and harmonic vibrational wavenumbers of MoN_2. Bond lengths in picometres. Roman numerals defining the structures refer to Fig. 1

Structure	ΔE/kJ mol^{-1}	$2S+1$	Point group[a]	Configuration[b]	Harmonic vibrational wavenumbers (assignment) This work	From ref. 12[c]	From ref. 11
(i)[d]	0	7 (Mo)	R_3 (Mo)	d^5s^1 (Mo)	2353 (N_2)	2363	
		0 (N_2)	$D_{\infty h}$ (N_2)	$\pi_u^4\sigma_g^2$ (N_2)	(exp 2359)		
(ii)	+0.84	7	$C_{\infty v}$	$\pi_\alpha^2\pi_\beta^2\sigma_\alpha^1\sigma_\beta^1\sigma_\alpha^1\delta_\alpha^2\pi_\alpha^2\sigma_\alpha^1$	70 (π)		
					17 (σ)		
					2343 (σ)		
(iii)	+1.26	5	$C_{\infty v}$	$\pi_\alpha^2\pi_\beta^2\sigma_\alpha^1\sigma_\beta^1\pi_\alpha^2\sigma_\alpha^1\delta_\alpha^2\pi_\beta^1$	303 (π)	322 (π)	
					497 (σ)	505 (σ)	
					1952 (σ)	2003 (σ)	
(iv)	+2.72	5	C_{2v}	$a_{1\beta}a_{1\alpha}b_{1\alpha}b_{1\beta}a_{1\alpha}a_{1\beta}b_{2\alpha}a_{1\alpha}a_{2\alpha}b_{1\alpha}a_{1\alpha}b_{2\beta}$	463 (a_1)		
					497 (b_2)		
					1684 (a_1)		
(v)	+20.92	3	C_{2v}	$a_{1\alpha}a_{1\beta}b_{2\alpha}a_{2\alpha}b_{2\beta}b_{1\alpha}a_{2\beta}b_{1\beta}a_{1\alpha}a_{1\beta}b_{2\alpha}a_{1\alpha}$	347 (a_1)	347 (a_1)	
					768 (b_2)	814 (b_1)	
					1005 (a_1)	1032 (a_1)	
(vi)	+42.43	1	C_{2v}	$a_1^2b_2^2a_2^2b_1^2a_1^2b_2^2$	457 (a_1)	469 (a_1)	
					924 (b_2)	990 (b_1)	
					1041 (a_1)	1078 (a_1)	
(vii)	+76.69	3	$C_{\infty v}$	$\pi_\beta^2\pi_\alpha^2\sigma_\beta^1\sigma_\alpha^1\sigma_\alpha^1\delta_\alpha^2\pi_\alpha^1\pi_\beta^2$	294 (π)		
					522 (σ)		
					1836 (σ)		
(viii)	+120.88	1	C_{2v}	$b_1^2a_1^2a_1^2b_2^2a_2^2a_1^2$	504 (a_1)		461 (a_1)
					776 (b_2)		896 (b_2)
					1078 (a_1)		1025 (a_1)

[a] All molecular geometries were optimised within the constraint of the point group shown. For C_{2v} symmetric species the molecular plane is the *yz* plane. [b] Electronic configuration of the 12 valence electrons (formally the 6 metal valence electrons and the 6 N p electrons). α and β notation designates electron spin in unrestricted calculations. Unless otherwise indicated, all MOs are singly occupied. [c] The molecular plane is the *xz* plane and hence b_1 and b_2 are interchanged. [d] Experimental N–N distance in free N_2 is 109.8 pm.

restricted formalism was employed for calculations on these states. For all states with $2S+1>1$, the spin unrestricted approach was used (*i.e.* an α spin electron in a molecular orbital of a given symmetry and number was not constrained to have the same spatial wavefunction as the corresponding β spin electron). The adjustable parameter controlling the numerical integration accuracy was set to 5.0 for geometry optimisations and 6.0 for frequency calculations. Mulliken population analyses were performed.[19] Molecular orbital plots were generated using the program MOLDEN, written by G. Schaftenaar of the CAOS/CAMM Centre, Nijmegen, The Netherlands.[20] The ADF output files (TAPE21) were converted to MOLDEN format using the program ADFrom written by F. Mariotti of the University of Florence.[20] The calculations were performed on IBM RS/6000 and Digital 433au workstations.

Results and discussion

A MoN_2

As mentioned in the Introduction, the principal focus of the present work is the interaction of an N_2 molecule with a U atom. However, in order to validate our methodology by comparison with previous theoretical studies, we have also investigated the analogous MoN_2 system. These results are now briefly discussed.

The optimised geometries and relative energies of MoN_2 are given in Fig. 1, with additional details in Table 1. In general, our data are similar to the *ab initio* CASPT2 results of Pyykkö and Tamm (compare Fig. 1 with Fig. 2 of ref. 11), with the exception of the relative energies of the quintet structures ((iii) and (iv)), which are reversed in order and are much more stable with respect to dissociation than at the CASPT2 level, and the spatial symmetry of the wide angle singlet structure (vi), which Pyykkö and Tamm find to be $^1B_2$ but which we determine as $^1A_1$. Martínez *et al.*[12] also find this structure to be of $^1A_1$ symmetry in their DFT studies (geometries calculated within the non-relativistic local density approximation (LDA) plus gradient corrected energies at the LDA stationary points) and their results are in general similar to ours, although they do not report the narrow angle high energy singlet structure.

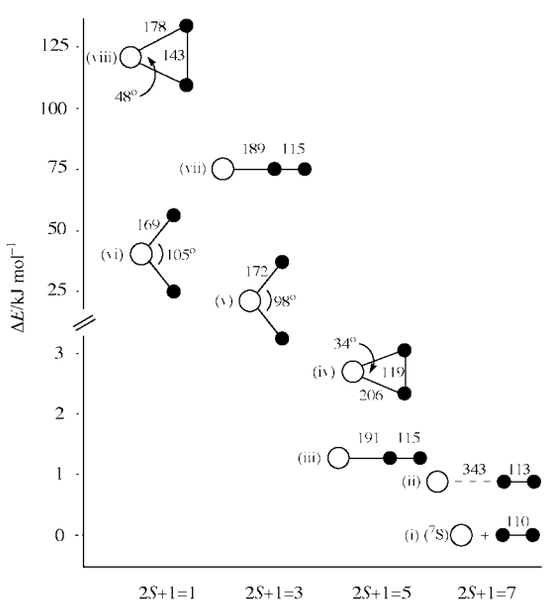

Fig. 1 Optimised geometries and relative energies of MoN_2 in different spin multiplicities. Bond lengths in picometres. Roman numerals beside each structure refer to Table 1.

Interestingly, Martínez *et al.*[12] predict that both quintet structures should be lower in energy than dissociated Mo and N_2, and note that this result may arise from the well-known DFT tendency to overbinding. Certainly Pyykkö and Tamm's[11] CASPT2 placement of these structures at 65–85 kJ mol^{-1} above the dissociation limit supports this assertion. Our DFT results, which differ from those of Martínez *et al.*[12] in that (a) gradient

Table 2 Molecular structures, relative energies, spin states, symmetries, valence electronic configurations and harmonic vibrational wavenumbers of UN_2. Bond lengths in picometres. Roman numerals defining the structures refer to Fig. 2

Structure	ΔE/ kJ mol^{-1}	$2S+1$	Point group[a]	Configuration[b]	Harmonic vibrational wavenumbers (assignment) This work	From ref. 22	From ref. 26	From ref. 21 (exp)
(i)[c]	0	5 (U) 0 (N_2)	R_3 (U) $D_{\infty h}$ (N_2)	$f^3d^1s^2$ (U) $\pi_u^4\sigma_g^2$ (N_2)	See Table 1			
(ii)	−133.25	3	C_s	$a''_\beta a'_\alpha a'_\beta a''_\alpha a'_\beta a'_\alpha a'_\alpha a'_\beta a'_\alpha a''_\alpha a''_\beta$	243 (a′)[d] 278 (a′) 1790 (a′)			
(iii)	−140.17	7	C_{2v}	$a_{1\alpha}b_{1\alpha}b_{1\beta}a_{1\beta}a_{1\alpha}a_{1\beta}b_{2\alpha}a_{1\alpha}a_{2\alpha}a_{2\alpha}b_{1\alpha}a_{1\alpha}$	347 (b_2) 361 (a_1) 1585 (a_1)			
(iv)	−142.89	5	C_{2v}	$a_{1\alpha}b_{1\alpha}b_{1\beta}a_{1\beta}a_{1\alpha}a_{1\beta}b_{2\alpha}a_{1\alpha}a_{1\beta}a_{2\alpha}b_{1\alpha}a_{1\alpha}$	242 (a_1) 252 (b_2) 1812 (a_1)			
(v)	−154.32	7	C_s	$a''_\alpha a'_\alpha a'_\beta a''_\beta a'_\alpha a'_\beta a'_\alpha a''_\alpha a'_\alpha a''_\alpha a'_\alpha a''_\alpha$	260 (a′)[e] 272 (a″) 382 (a′) 1646 (a′)			
(vi)	−412.54	3	C_{2v}	$a_{2\alpha}b_{2\alpha}b_{2\beta}a_{2\beta}a_{1\alpha}b_{1\alpha}a_{1\alpha}a_{1\beta}b_{1\beta}a_{1\beta}b_{2\alpha}a_{1\alpha}$	119 (a_1) 853 (b_2) 912 (a_1)			
(vii)	−540.47	1	$D_{\infty h}$	$\pi_g^4\pi_u^4\sigma_g^2\sigma_u^2$	61 (π_u) 1049 (σ_g) 1089 (σ_u)	53 (π_u) 1087 (σ_g) 1123 (σ_u)	245 (π_u) 1168 (σ_g) 1209 (σ_u)	 1008 (σ_g) 1051 (σ_u)

[a] All molecular geometries were optimised within the constraint of the point group shown. $C_{\infty v}$ structures were calculated in C_s symmetry to aid convergence. For C_{2v} symmetric species the molecular plane is the *yz* plane. [b] Electronic configuration of the 12 valence electrons (formally the 6 metal valence electrons and the 6 N p electrons). α and β notation designates electron spin in unrestricted calculations. Unless otherwise indicated, all MOs are singly occupied. [c] Experimental N–N distance in free N_2 is 109.8 pm. [d] Optimised bond angle is 179.7° hence 3 vibrational wavenumbers. [e] Optimised bond angle is 180.0° hence 4 vibrational wavenumbers.

corrections have been included self-consistently throughout the geometry optimisations and (b) relativistic corrections have been employed, place these structures at energies in between those of Martínez *et al.*[12] and Pyykkö and Tamm,[11] although both structures are still very close to the dissociation limit.

Table 1 includes the calculated vibrational wavenumbers of the MoN_2 structures, together with previous computational data. Data for free N_2 are also given, from which it may be seen that the agreement between theory and experiment is very good. We are not aware of any published experimental data for the MoN_2 species and hence, like previous workers,[11,12] we hope that our calculated wavenumbers will find use in future experiments. We note that there are no imaginary vibrational modes for any of the calculated structures, and hence that all of them are true minima on their respective potential energy surfaces.

Both Martínez *et al.*[12] and Pyykkö and Tamm[11] discuss the bonding in the various MoN_2 complexes. We concur with these analyses and have nothing to add, except to note that we will adopt a similar approach in our discussions of UN_2. We therefore leave MoN_2, noting that our calculations agree well with previous DFT and *ab initio* studies, thereby giving us confidence for our investigations of the interaction of N_2 with U.

B UN_2

The optimised geometries and relative energies of UN_2 are given in Fig. 2, with additional details in Table 2. All of these stationary point structures have been characterised as true energy minima by harmonic vibrational analysis. As with MoN_2 we find both end-on and side-on coordination of N_2 to the metal, although the distribution of these structures over the spin states is quite different in the actinide system. For example, there is a side bound UN_2 complex for $2S+1 = 7$ which has no MoN_2 equivalent, and the transition metal system has an end-on quintet structure that is not found for UN_2. Also noticeable is the lack of any UN_2 complex for $2S+1 = 1$ other than linear NUN, which has no Mo analogue. By contrast with MoN_2, all of the UN_2 minima are located below the dissociation limit,

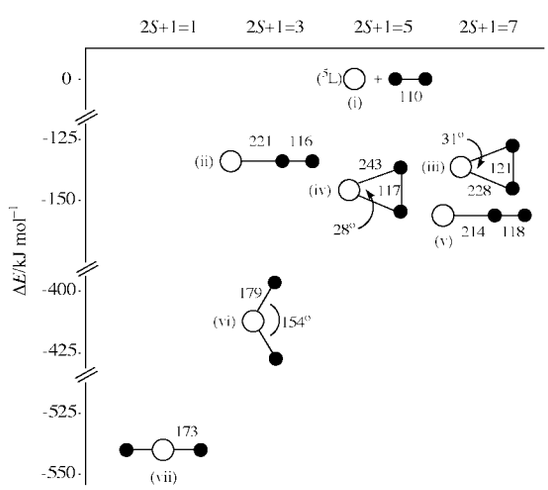

Fig. 2 Optimised geometries and relative energies of UN_2 in different spin multiplicities. Bond lengths in picometres. Roman numerals beside each structure refer to Table 2.

indicating that UN_2 is stable with respect to U + N_2. One UN_2 structure is certainly known experimentally, linear NUN being one of the primary products of the reaction between laser ablated U atoms and dinitrogen.[21,22]

(i) Spin–orbit coupling. All of the structures in Fig. 2 and Table 2 have been calculated at the scalar relativistic level, *i.e.* the effects of spin–orbit coupling have not been taken into account. While this approach is not expected to produce significant errors for MoN_2, spin–orbit coupling is sufficiently large in the actinide elements that it may well affect the present study. Application of the Russell–Saunders coupling scheme to atomic U yields a ^5L[23] ground term, with five levels characterised by $J = 6$ (most stable), 7, 8, 9 and 10. Unfortunately the present computational approach does not allow us to calculate the energies of the *J* levels.

Table 3 Principal contributors and bonding characteristics of the 12 highest occupied molecular orbitals of narrow angle quintet UN_2

Molecular orbital[a]	Principal components	Bonding character
$a_{1\alpha}$-HOMO	U f	Non
$b_{1\alpha}$	U f	Non
$a_{2\alpha}$	U f/N_2 out of plane π_g	U–N_2 δ[b]/N–N π^*
$a_{1\beta}$	U s	Non
$a_{1\alpha}$	U s	Non
$b_{2\alpha}$	N_2 in plane π_g/U f + d	N–N π^*/U–N_2 π[b]
$a_{1\beta}$	N_2 σ	N–N σ
$a_{1\alpha}$	N_2 σ	N–N σ
$a_{1\beta}$	N_2 in plane π_u	N–N π
$b_{1\beta}$	N_2 out of plane π_u	N–N π
$b_{1\alpha}$	N_2 out of plane π_u	N–N π
$a_{1\alpha}$	N_2 in plane π_u	N–N π

[a] All MOs are singly occupied. [b] Symmetry with respect to the principal axis.

Pyykkö and Tamm were faced with a similar problem when extending their MoN_2 studies to WN_2,[11] and adopted a semi-empirical approach to determine the energy of the $^5D_0$ ground level of W. They took the $^5D_0$ energy to be that of the calculated ^7S first excited state minus the experimental $^7S \leftarrow {}^5D_0$ transition energy. Unfortunately this approach does not work for U because an analogous transition to an excited S term is not well established (indeed, the assignment of the atomic spectrum of U is far from complete).

We can make progress by noting that (a) the use of the Russell–Saunders scheme to treat actinide spin–orbit coupling is at best debateable[24] and (b) ADF has the facility to apply a spin–orbit operator in single point calculations such that the electronic wavefunctions form bases for one of the irreducible representations of the atomic or molecular double point group.[25] Adopting this approach to atomic U lowers the energy with respect to the ^5L term by 137 kJ mol^{-1}, and hence the energy of the U + N_2 asymptote should be stabilised by this amount. However, single point double group calculation of linear NUN at the optimised scalar relativistic geometry yields a stabilisation of 177 kJ mol^{-1} with respect to the scalar structure, and hence the inclusion of spin–orbit coupling does not greatly alter the energy of NUN with respect to the U + N_2 asymptote. Unfortunately it was not possible to converge single point double group calculations on the other UN_2 stationary point structures given in Fig. 2 and Table 2, and thus we cannot determine if spin–orbit coupling would alter the relative energies of these minimum energy structures. We therefore proceed to analyse the bonding in the scalar minima noting that, to the best of our knowledge, spin–orbit coupling does not significantly alter the energy of the UN_2 stationary point structures relative to the U + N_2 asymptote.

(ii) Bonding analyses. *(a) The narrow angle triangular structures.* We can understand the bonding in the UN_2 complexes by considering the interaction of the six metal valence electrons (*i.e.* those outside the [Rn] core) with the six electrons in the 2p orbitals of the N atoms, thereby setting up a 12 electron problem. Fig. 2 indicates that there are two narrow angle triangular UN_2 structures, a septet (iii) and a quintet (iv), which have very similar energies and which may be regarded as containing a side-on chemical bond to a partly dissociated N_2 molecule. The configuration of the 12 valence electrons in the quintet complex (iv) is $a_{1\alpha}b_{1\alpha}b_{1\beta}a_{1\beta}a_{1\alpha}a_{1\beta}b_{2\alpha}a_{1\alpha}a_{1\beta}a_{2\alpha}b_{1\alpha}a_{1\alpha}$. The principal components and bonding characteristics of these MOs are collected in Table 3, and pictures of the $b_{2\alpha}$ and $a_{2\alpha}$ orbitals are shown in Fig. 3 (a) and (b) respectively. The 12 MOs may be divided into two groups of six. The more stable six are essentially the N_2 π and σ bonding MOs. The higher lying six orbitals have predominant metal character, with only two MOs, $b_{2\alpha}$ and $a_{2\alpha}$, showing any significant metal/N_2 mixing. In both of these MOs the N_2 contribution is from the N–N π_g antibonding orbitals, indicating that the binding of the N_2 molecule to the U occurs *via* metal$\rightarrow N_2$ backbonding. Consistent with this are the calculated atomic charges, +0.32 and −0.16 respectively for U and N, as well as the U–N overlap population, +0.26 electrons.

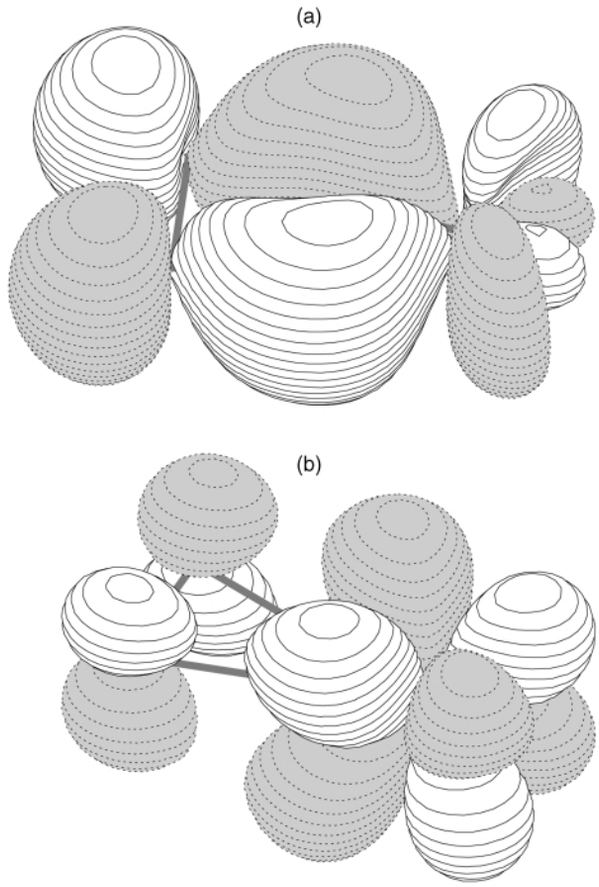

Fig. 3 The (a) $b_{2\alpha}$ and (b) $a_{2\alpha}$ molecular orbitals of narrow angle triangular quintet UN_2 (structure (iv)).

It is noticeable that the metal$\rightarrow N_2$ backbonding is both qualitatively and quantitatively different in the $b_{2\alpha}$ and $a_{2\alpha}$ MOs. The $b_{2\alpha}$ orbital is clearly π backbonding, while the equivalent interaction in the $a_{2\alpha}$ level is of δ symmetry with respect to the principal molecular axis. Furthermore, the π interaction is stronger than the δ, as evidenced by the contribution of the N_2 π_g MO to the $b_{2\alpha}$ and $a_{2\alpha}$ MOs (*ca.* 50% and *ca.* 14% respectively). This conclusion is also supported by Fig. 3, which demonstrates a greater U/N_2 mixing in the $b_{2\alpha}$ level (both pictures have the same MOLDEN 'space' value, 0.05).

The electronic configuration of the narrow angle septet structure is similar to that of the quintet, differing only in the replacement of the highest lying quintet $a_{1\beta}$ MO by an $a_{2\alpha}$ orbital. The U–N distance is significantly shorter than in the quintet, and the N–N distance slightly longer. The population analysis is consistent with these observations, indicating stronger U–N bonding and reduced N–N bonding. Thus the calculated charges are +0.48 and −0.24 respectively for U and N (indicating greater transfer of charge from metal to N_2 than in the quintet case), the U–N overlap population is +0.39 electrons (up 0.13) and that between the N atoms is 0.15 electrons less than in the quintet.

(b) The wide angle triangular and linear NUN structures. As the spin state is reduced there is a trend toward increasing NUN angle and decreasing U–N distance. The wide angle structures cannot be considered as containing a slightly perturbed N_2 moiety (the N–N distance is 3.48 Å in the wide angle triplet structure (vi)) and, following Pyykkö and Tamm,[11] it is best to

Table 4 Principal contributors and bonding characteristics of the 12 highest occupied molecular orbitals of wide angle triplet UN_2

Molecular orbital[a]	Principal components[b]	Bonding character
$a_{1\alpha}$-HOMO	U f	Non
$b_{2\alpha}$	U f/N σ_-	U–N σ
$a_{1\beta}$	U f/N in plane π_+	U–N π
$b_{1\beta}$	U f/N out of plane π_+	U–N π
$a_{1\beta}$	N σ_+	U–N σ*
$a_{1\alpha}$	U f/N in plane π_+	U–N π
$b_{1\alpha}$	U f/N out of plane π_+	U–N π
$a_{1\alpha}$	N σ_+	U–N σ*
$a_{2\beta}$	N out of plane π_-	U–N π
$b_{2\beta}$	N in plane π_-	U–N π
$b_{2\alpha}$	N in plane π_-	U–N π
$a_{2\alpha}$	N out of plane π_-	U–N π

[a] All MOs are singly occupied. [b] N atomic orbital combinations defined in Fig. 4.

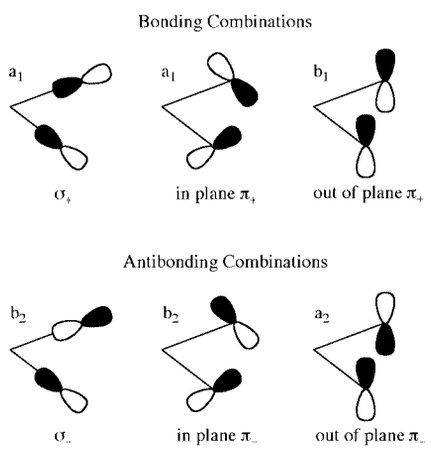

Fig. 4 Possible combinations of the 2p atomic orbitals of the nitrogen atoms in wide angle triplet UN_2 (structure (vi)).

treat the bonding at these geometries using a local co-ordinate system. Thus each N atom has a single pσ atomic orbital (*i.e.* one oriented along the U–N axis) and two pπ levels (perpendicular to the U–N axis), one oriented in the molecular plane and one perpendicular to it. These three p AOs can be coupled in a constructive and destructive manner with the equivalent orbitals on the second N to give the six combinations shown in Fig. 4.

The principal components and bonding character of the 12 highest occupied MOs of the wide angle triplet structure are given in Table 4. There are eight orbitals which are π bonding between the U and the N atoms, plus two σ* levels, one σ and one non-bonding MO (the HOMO). Simplistically we can say that there are seven net U–N bonding electrons, giving an approximate U–N bond order between 1.5 and 2. Mulliken analysis shows that the U–N overlap population is +1.42 electrons, greatly increased from the narrow angle cases. Consistent with the formal trend toward filling of the N 2p shell with U valence electrons, there is a significantly greater transfer of charge from U to N in the wide angle triplet, with the calculated atomic charges being +1.34 and −0.67 for U and N respectively.

Fig. 2 and Table 2 indicate that the most stable UN_2 structure is the linear NUN singlet. This structure is significant because linear NUN is isoelectronic with the uranyl ion (UO_2^{2+}) that is so ubiquitous in U chemistry. Linear NUN has been previously investigated computationally by two groups. Kushto *et al.* used methodology similar to that employed in the present study to determine a U–N bond length of 1.717 Å,[22] slightly longer than the 1.682 Å found by Pyykkö *et al.* at the Hartree–Fock level[26] (Pyykkö and Zhao also reported an earlier study of NUN at the Hartree–Fock and MP2 levels,[27] but this is misleading in that the calculations were accidentally performed on an excited state[28]). Our value of 1.734 Å is in good agreement with these previous studies. It is encouraging to note that our calculated vibrational wavenumbers (Table 2) show better agreement with experiment[21] than either of the previous computational studies, with a *ca.* 40 cm^{-1} overestimate of the σ_g and σ_u modes (the wavenumber of the low energy π_u mode has not been determined experimentally).

All 12 of the valence electrons of NUN (electronic configuration $\pi_g^4\pi_u^4\sigma_g^2\sigma_u^2$) are bonding between the U and the N (the g and u MOs with the U 6d and 5f AOs respectively) giving a formal U–N bond order of three. This increased bond order in comparison with the wide angle triplet structure is reflected in an increased U–N Mulliken overlap population, +1.62 electrons. The calculated atomic charges in the linear singlet structure are the same as for the bent triplet.

(c) The end-on structures. Fig. 2 and Table 2 indicate that there are two UN_2 complexes in which the N_2 unit is bonded in an end-on fashion to the metal. Analysis of the 12 highest occupied MOs of the septet structure (v) reveals that there are four orbitals which involve U/N mixing. The most significant U–N interaction is π backbonding from the U 5f orbitals into the N_2 π_g MOs, and there is a lesser σ interaction which is largely N-localised and which is antibonding between U and N. The calculated atomic charges show a significant electron transfer from U to N_2, being +0.54, −0.41 and −0.13 for U–N1–N2 respectively. The U–N1 Mulliken overlap population is +0.92 electrons, significantly greater than the narrow angle structures but less than the wide angle complexes, while the N–N population is +1.02 electrons, reduced from the +1.29 electrons calculated for free N_2. This is entirely consistent with the increased N–N distance in the end-on complex in comparison with N_2.

The remaining UN_2 species is the end-on coordinated triplet (ii) which is much less stable than the wide angle triplet structure. This complex has a longer U–N1 but shorter N–N distance than the analogous septet structure. Mulliken analysis is consistent with reduced U–N_2 bonding in the triplet species, with a U–N1 overlap population of +0.81 electrons and calculated charges of +0.44, −0.35 and −0.09 for U, N1 and N2 respectively.

Conclusions

The present study has identified multiple true energy minima on the potential energy surfaces of MoN_2 and UN_2 in spin multiplicities ranging from one to seven. There are three different structural types common to both metals, end-on co-ordinated N_2 plus narrow and wide angle triangular structures, and the UN_2 system also has a linear singlet NUN geometry which is by far the most stable. All of the UN_2 potential energy minima are predicted to be stable with respect to dissociation to U + N_2; by contrast none of the stationary point structures of MoN_2 lies below the metal + dinitrogen dissociation asymptote.

As discussed in the Introduction, much of the impetus for conducting this study stemmed from our previous calculations of $[\{(NH_2)_3(NH_3)U\}_2(\mu\text{-}\eta^2\text{:}\eta^2\text{-}N_2)]$[9,10] and related compounds. What, then, can we take from UN_2 to the triamidoamine system and its computational models? First, the present work confirms that there may be several stationary point structures, and that the molecular spin state is a key factor in determining the geometry adopted. Second, the bonding between U and side-on co-ordinated narrow angle N_2 is exclusively U 5f→N_2 π_g backbonding. For UN_2 this backbonding is a mixture of π (main interaction) and δ (secondary interaction) with respect to the principal molecular axis, whereas for $[\{(NH_2)_3(NH_3)U\}_2(\mu\text{-}\eta^2\text{:}\eta^2\text{-}N_2)]$ no δ interaction was found.[9] This may well reflect the formal oxidation state of the metal in the two systems, for it might be expected that there would be less backbonding in the

formally U(III) [{$(NH_2)_3(NH_3)U$}$_2$(μ-η^2:η^2-N_2)], leading to a negligible δ interaction.

The present study clearly supports our previous conclusion that the side-on interaction of U with N_2 is predominantly *via* metal→dinitrogen backbonding. Unfortunately this result does not resolve the puzzle of the N–N distance in the triamido-amine diuranium dinitrogen compound, as the π backbonding in the present calculations is always accompanied by an N–N lengthening. Work on this problem is continuing.

Acknowledgements

We are grateful to the EPSRC for a PhD studentship (to KLB), the Royal Society and the University of London's Central Research Fund for equipment grants and Professor Pekka Pyykkö for helpful discussions.

References

1 M. B. O'Donoghue, N. C. Zanetti, W. M. Davis and R. R. Shrock, *J. Am. Chem. Soc.*, 1997, **119**, 2753.
2 M. B. O'Donoghue, W. M. Davis and R. R. Shrock, *Inorg. Chem.*, 1998, **37**, 5149.
3 N. Desmangles, H. Jenkins, K. B. Ruppa and S. Gambarotta, *Inorg. Chim. Acta*, 1996, **250**, 1.
4 J. D. Cohen, M. D. Fryzuk, T. M. Loehr, M. Mylvaganam and S. J. Rettig, *Inorg. Chem.*, 1998, **37**, 112.
5 J. Jubb and S. Gambarotta, *J. Am. Chem. Soc.*, 1994, **116**, 4477.
6 E. Campazzi, E. Solari, C. Floriani and R. Scopelliti, *Chem. Commun.*, 1998, 2603.
7 A. L. Odom, P. L. Arnold and C. C. Cummins, *J. Am. Chem. Soc.*, 1998, **120**, 5836.
8 P. Roussel and P. Scott, *J. Am. Chem. Soc.*, 1998, **120**, 1070.
9 N. Kaltsoyannis and P. Scott, *Chem. Commun.*, 1998, 1665.
10 N. Kaltsoyannis and P. Scott, *Abstr. Pap. Am. Chem. Soc.*, 1999, **217**, 117-NUCL.
11 P. Pyykkö and T. Tamm, *J. Phys. Chem. A*, 1997, **101**, 8107.
12 A. Martínez, A. M. Köster and D. R. Salahub, *J. Phys. Chem. A*, 1997, **101**, 1532.
13 G. te Velde and E. J. Baerends, *J. Comput. Phys.*, 1992, **99**, 84.
14 ADF⟨2.3⟩, Department of Theoretical Chemistry, Vrije Universiteit, Amsterdam, 1997.
15 T. Ziegler, V. Tschinke, E. J. Baerends, J. G. Snijders and W. Ravenek, *J. Phys. Chem.*, 1989, **93**, 3050.
16 S. H. Vosko, L. Wilk and M. Nusair, *Can. J. Phys.*, 1980, **58**, 1200.
17 A. Becke, *Phys. Rev. A.*, 1988, **38**, 3098.
18 J. P. Perdew, *Phys. Rev.*, 1986, **B33**, 8822.
19 R. S. Mulliken, *J. Chem. Phys.*, 1955, **23**, 1833, 1841, 2338, 2343.
20 For details of both MOLDEN and ADFrom, the reader is directed to http://www.caos.kun.nl/~schaft/molden/molden.html
21 R. D. Hunt, J. T. Yustein and L. Andrews, *J. Phys. Chem.*, 1993, **98**, 6070.
22 G. P. Kushto, P. F. Souter and L. Andrews, *J. Chem. Phys.*, 1998, **108**, 7121.
23 C. C. Keiss, C. J. Humphreys and D. D. Laun, *J. Res. Nat. Bur. Stand.* (*U.S.*), 1946, **37**, 57.
24 N. Kaltsoyannis and P. Scott, *The f elements*, Oxford University Press, Oxford, 1999.
25 N. Kaltsoyannis, *J. Chem. Soc.*, *Dalton Trans.*, 1997, 1.
26 P. Pyykkö, J. Li and N. Runeberg, *J. Phys. Chem.*, 1994, **98**, 4809.
27 P. Pyykkö and Y. Zhao, *Inorg. Chem.*, 1991, **30**, 3787.
28 P. Pyykkö, personal communication.

Paper 9/07864I